

April 9, 2019

Decreasing the size of the Restricted Boltzmann machine

Yohei Saito^{1,*} and Takuya Kato^{2,†}

¹*Institute of Industrial Science, The University of Tokyo,
4-6-1, Komaba, Meguro-ku, Tokyo 153-8505 Japan*

²*Graduate School of Information Science and Technology,
Department of Mathematical informatics, The University of Tokyo,
7-3-1, Hongo, Bunkyo-ku, Tokyo 113-8654, Japan*

We propose a method to decrease the number of hidden units of the restricted Boltzmann machine while avoiding decrease of the performance measured by the Kullback-Leibler divergence. Then, we demonstrate our algorithm by using numerical simulations.

I. INTRODUCTION

Improvement of computer performance enables utilization of exceedingly high representational powers of neural networks, which leads to great success of deep neural networks both in discrimination and generation of data, e.g. images, speech, and natural language [1–5]. In order to increase performance, which stems from hierarchical structures of neural networks [6], network size becomes larger and larger, and computational burdens increase. Thus, demands for decreasing network size are growing, and in particular, various methods were proposed for compressing sizes of discriminative models [7–9]. However, compression of generative models [10] has scarcely been discussed.

Discriminative models provide probabilities that into which class given data are classified [11], and in most cases, their learning requires a supervisor, namely, a dataset attached classification labels by humans. Thus, outputs of discriminative models can be intuitively interpreted by humans. However, some data are difficult for humans to find useful classification, and if it can be found, hand-labeling tasks are troublesome labor. In such cases, generative models with unsupervised learning effectively work, since they automatically find data structure without hand-labels by learning joint probabilities of data and classes, which may not easily be interpreted by humans. Therefore, it can be expected that compression of generative models with unsupervised learning will be required in future. Furthermore, if performance of a system can be preserved in a process of compression, one can decrease network size while continuing to use it. Thus, in order to approximately keep performance

throughout a process of compression, we consider to remove a part of a system after decreasing its contribution to performance, unlike the procedures in previous studies [7–10], which retrain systems after removing a part of systems which contributes little to their performance. Since the definition of performance depends on details of models and objectives, we do not treat general generative models, but deal with the restricted Boltzmann machine (RBM) [12, 13], which is one of the most important generative models with unsupervised learning, from the viewpoints of machine learning history [1] and its wide applications, e.g., generation of new samples, classification of data [14], feature extraction [15], pre-training of deep neural networks [15–17], and solving many-body problems in physics [18, 19].

The RBM is constituted by visible units which represent components of observables, e.g., pixels of images, and hidden units which express correlation between visible units. An objective of the RBM is to generate plausible data by imitating the probability from which true data are sampled. Therefore, in this case, the performance of the RBM is quantified by the difference between the probability distribution of data and that of visible variables of the RBM, such as Kullback-Leibler divergence (KLD). It was shown that the RBM can exactly reproduce any probability distribution of binary data, if it has plenty number of hidden units [20]. However, a smaller number of hidden units may be enough to express some kinds of probability according to data structure. Therefore, in this paper, we aim to decrease the number of hidden units practically while avoiding increase of the KLD (Fig. 1).

The outline of this paper is as follows. In Section 2, we give a brief review of the RBM. In Section 3, we evaluate deviation of the KLD associated with node removal and propose a method which decreases the number of the hidden units while avoiding increase

* yoheis@sat.t.u-tokyo.ac.jp

† takuya.kato.origami@gmail.com

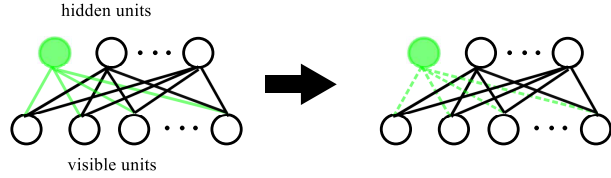


FIG. 1. The graphical model of the RBM is shown. While approximately preserving the KLD, the target hidden unit and its edges (green) are removed from the main body of the RBM (from the left to the right panel).

of the KLD. In Section 4, we demonstrate numerical simulations, and in Section 5, we summarize this paper. The details of calculations are shown in Appendices.

II. BRIEF INTRODUCTION OF THE RBM

In this Section, we briefly review the RBM. The RBM is a kind of Markov random field, and is constituted by visible units, $\mathbf{v} = (v_1, \dots, v_M) \in \{0, 1\}^M$, and hidden units, $\mathbf{h} = (h_1, \dots, h_N) \in \{0, 1\}^N$. The joint probability that a configuration (\mathbf{v}, \mathbf{h}) is realized, $p(\mathbf{v}, \mathbf{h})$, is given by the energy function, $E(\mathbf{v}, \mathbf{h})$, as follows:

$$\begin{aligned} E(\mathbf{v}, \mathbf{h}) &= -\mathbf{b}^T \mathbf{v} - \mathbf{c}^T \mathbf{h} - \mathbf{v}^T W \mathbf{h} \\ &= -\sum_{i=1}^M b_i v_i - \sum_{j=1}^N c_j h_j \\ &\quad - \sum_{i=1}^M \sum_{j=1}^N v_i w_{ij} h_j, \end{aligned} \quad (1)$$

$$p(\mathbf{v}, \mathbf{h}) = \frac{e^{-E(\mathbf{v}, \mathbf{h})}}{\sum_{\mathbf{v}', \mathbf{h}'} e^{-E(\mathbf{v}', \mathbf{h}')}}, \quad (2)$$

where $\mathbf{b} = (b_1, \dots, b_M) \in \mathbb{R}^M$ and $\mathbf{c} = (c_1, \dots, c_N) \in \mathbb{R}^N$ are biases of visible and hidden units, respectively, and $W = (w_{ij}) \in \mathbb{R}^{M \times N}$ is the weight matrix [21]. Below, we abbreviate all of the RBM parameters, \mathbf{b} , \mathbf{c} , and W , as ξ .

By properly tuning ξ , the probability distribution of the visible variables, $p(\mathbf{v}) = \sum_{\mathbf{h}} p(\mathbf{v}, \mathbf{h})$, can approximate unknown probability that generates real data, $q(\mathbf{v})$, and performance of the RBM can be measured by KLD of $p(\mathbf{v})$ from $q(\mathbf{v})$,

$$D_{\text{KL}}(q||p) = \sum_{\mathbf{v}} q(\mathbf{v}) \ln \frac{q(\mathbf{v})}{p(\mathbf{v})}. \quad (3)$$

Hence, learning of the RBM is performed by updating the RBM parameters ξ so as to decrease the KLD. The gradient descent method is often employed to

decrease the KLD as

$$\xi^{s+1} = \xi^s - \lambda \nabla_{\xi} D_{\text{KL}}(q||p)|_{\xi=\xi^s}, \quad (4)$$

where ξ^s and ξ^{s+1} denote the RBM parameters at s -th and $(s+1)$ -th step of the learning process, respectively. A learning rate is represented by $\lambda (> 0)$, and $\nabla_{\xi} D_{\text{KL}}(q||p)|_{\xi=\xi^s}$ denotes the gradient of the KLD with respect to ξ at s -th step. The gradient with respect to b_i , c_j , and w_{ij} can be written as

$$\frac{\partial D}{\partial b_i} = -\sum_{\mathbf{v}} v_i q(\mathbf{v}) + \langle v_i \rangle_p, \quad (5)$$

$$\frac{\partial D}{\partial c_j} = -\sum_{\mathbf{v}} q(\mathbf{v}) p(h_j = 1|\mathbf{v}) + \langle h_j \rangle_p, \quad (6)$$

$$\frac{\partial D}{\partial w_{ij}} = -\sum_{\mathbf{v}} v_i q(\mathbf{v}) p(h_j = 1|\mathbf{v}) + \langle v_i h_j \rangle_p, \quad (7)$$

where we abbreviate $D_{\text{KL}}(q||p)$ as D and expectation value with respect to $p(\mathbf{v}, \mathbf{h})$ as $\langle \cdot \rangle_p$. The conditional probability, $p(h_j|\mathbf{v})$, is given by

$$p(h_j|\mathbf{v}) = \frac{e^{(c_j + \sum_i v_i w_{ij}) h_j}}{1 + e^{(c_j + \sum_i v_i w_{ij}) h_j}}. \quad (8)$$

If D and $\nabla_{\xi} D$ can be obtained, the RBM reaches some local minimum of the KLD through parameter update. However, neither of them can be calculated, since they contain not only unknown probability $q(\mathbf{v})$, but also sum with respect to large state space of the RBM. Thus, in Eqs. (5), (6) and (7), one approximates $q(\mathbf{v})$ by empirical distribution, or more practically, mini-batch, which are samples from empirical distribution, and also evaluates expectation values with respect to $p(\mathbf{v}, \mathbf{h})$, which are computationally expensive, by using realizations obtained from Gibbs sampling, e.g. contrastive divergence (CD) [22], persistent CD (PCD) [23], fast PCD [24], and block Gibbs sampling with tempered transition [25] or parallel tempering [26, 27]. Furthermore, the KLD, which represents the performance of the RBM, is also intractable. Therefore, in order to monitor the progress of learning, some different quantity is employed which can be considered to correlate to the KLD to a certain degree [28–32].

III. REMOVAL OF HIDDEN UNITS

A. Removal cost and its gradient

The goal of this paper is not to propose a new method for optimization of the KLD, but to decrease the number of the hidden units while avoiding increase of the KLD. Suppose an RBM achieves, if not optimal, sufficient performance after the learning process at a

fixed number of hidden units, N . Next, we remove k -th hidden unit of the RBM so as not to increase the KLD. In order to compare the performances of two RBMs whose k -th hidden unit does or does not exist, we introduce $\mathbf{h}_{\setminus k}$ as a configuration of hidden units except for h_k , $\mathbf{h}_{\setminus k} = (h_1, \dots, h_{k-1}, h_{k+1}, \dots, h_N)$. The energy function and the probability distribution of the RBM after removal are given by

$$\begin{aligned} E_{\setminus k}(\mathbf{v}, \mathbf{h}_{\setminus k}) &= -\sum_i b_i v_i - \sum_{j \neq k} c_j h_j \\ &\quad - \sum_i \sum_{j \neq k} v_i w_{ij} h_j \\ &= E(\mathbf{v}, \mathbf{h})|_{h_k=0}, \end{aligned} \quad (9)$$

$$p_{\setminus k}(\mathbf{v}, \mathbf{h}_{\setminus k}) = \frac{e^{-E_{\setminus k}(\mathbf{v}, \mathbf{h}_{\setminus k})}}{\sum_{\mathbf{v}', \mathbf{h}'_{\setminus k}} e^{-E_{\setminus k}(\mathbf{v}', \mathbf{h}'_{\setminus k})}}. \quad (10)$$

Then, we define a removal cost, C_k , as the difference of the KLD before and after removing k -th hidden unit:

$$\begin{aligned} C_k &\equiv D_{\text{KL}}(q||p_{\setminus k}) - D_{\text{KL}}(q||p) \\ &= \sum_{\mathbf{v}} q(\mathbf{v}) \ln \frac{q(\mathbf{v})}{p_{\setminus k}(\mathbf{v})} - \sum_{\mathbf{v}} q(\mathbf{v}) \ln \frac{q(\mathbf{v})}{p(\mathbf{v})} \\ &= -\sum_{\mathbf{v}} q(\mathbf{v}) \ln p(h_k = 0|\mathbf{v}) \\ &\quad + \ln p(h_k = 0). \end{aligned} \quad (11)$$

The detail of the calculation and a removal cost for several hidden units are shown in Appendix A. Thus, if C_k satisfies $C_k \leq 0$, k -th hidden unit can be removed without increasing the KLD.

In most cases, however, there are no hidden units whose removal costs are non-positive values. Thus, before removing a hidden unit, we first decrease its removal cost without increasing the KLD [33]. For this purpose, we naively determine parameter update at s -th step in a removal process, $\Delta\xi^s$, so that both C_k and the KLD decrease at $\mathcal{O}(|\Delta\xi^s|)$ (see Appendix B):

$$\Delta\xi_i^s = -\nu \cdot \theta \left(\frac{\partial D}{\partial \xi_i} \frac{\partial C_k}{\partial \xi_i} \right) \cdot \frac{\partial D}{\partial \xi_i} \Big|_{\xi=\xi^s}, \quad (12)$$

$$\theta(x) = \begin{cases} 1 & (x \geq 0) \\ 0 & (x < 0) \end{cases}, \quad (13)$$

where $\nu (> 0)$ is a parameter change rate, and $\theta(x)$ is the step function. One can evaluate $\nabla_{\xi} D$ from

Eqs. (5), (6) and (7), and $\nabla_{\xi} C_k$ can be written as

$$\frac{\partial C_k}{\partial b_i} = \langle v_i \rangle_{\bar{p}} - \langle v_i \rangle_p, \quad (14)$$

$$\begin{aligned} \frac{\partial C_k}{\partial c_j} &= \sum_{\mathbf{v}} q(\mathbf{v}) p(h_k = 1|\mathbf{v}) \delta_{kj} \\ &\quad + \langle h_j \rangle_{\bar{p}} - \langle h_j \rangle_p, \end{aligned} \quad (15)$$

$$\begin{aligned} \frac{\partial C_k}{\partial w_{ij}} &= \sum_{\mathbf{v}} q(\mathbf{v}) v_i p(h_k = 1|\mathbf{v}) \delta_{kj} \\ &\quad + \langle v_i h_j \rangle_{\bar{p}} - \langle v_i h_j \rangle_p, \end{aligned} \quad (16)$$

where δ_{kj} is the Kronecker delta, and $\langle \cdot \rangle_p$ and $\langle \cdot \rangle_{\bar{p}}$ mean expectation values with respect to $p(\mathbf{v}, \mathbf{h})$ and $\bar{p} \equiv p(\mathbf{v}, \mathbf{h}_{\setminus k} | h_k = 0)$, respectively. If $C_k \leq 0$ is satisfied after parameter updates, k -th hidden unit can be removed without increasing the KLD. When all of the RBM parameters satisfy $\partial D / \partial \xi_i \cdot \partial C_k / \partial \xi_i < 0$, C_k cannot decrease without increasing the KLD, and parameter update is stopped ($\Delta\xi = \mathbf{0}$) [34].

Here, we comment on two properties of C_k . First, $-C_k$ can be interpreted as an additional cost of a new node and may be employed when one adds new nodes into an RBM whose performance is insufficient. Secondly, Eq. (11) can be applied to the Boltzmann machine (BM) [35], which is expressed as a complete graph constituted by visible and hidden units, and a special case of the BM called deep Boltzmann machine (DBM) [36], which has hierarchical hidden layers with neighboring interlayer connections. However, in these cases, calculation of the conditional probability, $p(h_k = 0|\mathbf{v})$, and gradients with respect to the model parameters are computationally expensive compared to the RBM.

B. Practical removal procedure

The removal process proposed in the previous subsection preserves the performance when C_k , $\nabla_{\xi} C_k$, and $\nabla_{\xi} D$ can be accurately evaluated. In most cases, however, we approximate C_k and $\nabla_{\xi} C_k$ by using Gibbs sampling as with $\nabla_{\xi} D$. Thus, in order to reflect variances of Gibbs sampling, we change both parameter update rule and removal condition, Eqs. (12) and (11), into more effective forms.

First, we modify our parameter update rule, Eq. (12), which may increase D owing to the inaccuracy of Gibbs sampling or contribution to D from higher order terms, $\mathcal{O}(|\Delta\xi|^2)$. It is expected that the update rule, Eq. (12), eventually compensate the occasional increase of D caused by the above-listed two reasons, since the update rule is designed to decrease D at $\mathcal{O}(|\Delta\xi|)$. However, we found that the simple applica-

tion of the update rule could not compensate for the occasional increase. The reason is as follows: Since removal cost is defined as the change of the KLD through node removal, it can be interpreted as the contribution of the node to the performance. Hence, when the performance increases, removal costs are expected to increase, which means that in RBM parameter space, there are few directions along which both D and C_k decrease. Since the step function in Eq. (12) allows parameter update solely along these few directions, there are few opportunities to decrease D . Hence, in order to effectively decrease D , we heuristically change the step function in Eq. (12) into a form that allows increase of C_k to a certain extent by probabilistically accepting such updates. That is, we change the step function which gives either 0 or 1 deterministically into a random variable, $z_i \in \{0, 1\}$. Next, we determine the probability that z_i takes 1, namely, the acceptance probability of updates. We require that a modified update rule returns to Eq. (12), when Gibbs sampling estimates are exactly obtained. For this purpose, we employ the ratio of the mean to the standard deviation and determine the modified update rule by

$$\overline{\Delta \xi_i^s} = -\nu z_i \overline{\partial_i D} |_{\xi=\xi^s}, \quad (17)$$

$$p(z_i = 1) = \text{sig} \left(\frac{\sqrt{S} \cdot \overline{\partial_i D}}{\overline{\sigma_{D,i}}} \cdot \frac{\sqrt{S} \cdot \overline{\partial_i C_k}}{\overline{\sigma_{C,i}}} \right), \quad (18)$$

$$\text{sig}(x) = \frac{e^x}{1 + e^x}, \quad (19)$$

where S is the number of Gibbs samplers, $\overline{\partial_i D}$ and $\overline{\partial_i C_k}$ represent sample means of $\partial D / \partial \xi_i$ and $\partial C_k / \partial \xi_i$, respectively. The unbiased standard deviations of $\partial D / \partial \xi_i$ and $\partial C_k / \partial \xi_i$ are denoted by $\overline{\sigma_{D,i}}$ and $\overline{\sigma_{C,i}}$, respectively. As the number of samplers increases, Eq. (17) returns Eq. (12) [37].

Secondly, we modify our removal condition, Eq. (11). Since node removal irreversibly decreases the representational power of the RBM, we carefully verify whether $C_k \leq 0$ is satisfied. However, since the logarithmic function in the second term of Eq. (11) drastically decreases in $p(h_k = 0) < 1$, a small sampling error in $p(h_k = 0)$ results a large error in $\ln p(h_k = 0)$, which makes hard to evaluate removal cost accurately by Gibbs sampling. Therefore, we employ an upper

bound of C_k as an effective removal cost, C'_k :

$$\begin{aligned} C_k &= -\sum_{\mathbf{v}} q(\mathbf{v}) \ln p(h_k = 0 | \mathbf{v}) \\ &\quad + \ln[1 - p(h_k = 1)] \\ &\leq -\sum_{\mathbf{v}} q(\mathbf{v}) \ln p(h_k = 0 | \mathbf{v}) \\ &\quad - p(h_k = 1) \\ &\equiv C'_k. \end{aligned} \quad (20)$$

Then, consider approximation of C'_k by Gibbs sampling,

$$\begin{aligned} \overline{C'_k} &\equiv -\frac{1}{S} \sum_{\alpha=1}^S \ln p(h_k = 0 | \mathbf{v}^\alpha) \\ &\quad - \frac{1}{S} \sum_{\alpha=1}^S h_k^\alpha, \end{aligned} \quad (21)$$

where α is sample index. Since samplings from $q(\mathbf{v})$ and $p(\mathbf{v}, \mathbf{h})$ are independent, the first and second terms of Eq. (21) have no correlations. Thus, when the sampling size, S , is sufficiently large, the probability distribution of $\overline{C'_k}$ can be approximated by the normal distribution, due to the central limit theorem:

$$\overline{C'_k} \sim \mathcal{N} \left(C'_k, \frac{\sigma_1^2}{S} + \frac{\sigma_2^2}{S} \right), \quad (22)$$

$$\begin{aligned} \sigma_1^2 &= \sum_{\mathbf{v}} q(\mathbf{v}) [\ln p(h_k = 1 | \mathbf{v})]^2 \\ &\quad - \left[\sum_{\mathbf{v}} q(\mathbf{v}) \ln p(h_k = 1 | \mathbf{v}) \right]^2, \end{aligned} \quad (23)$$

$$\sigma_2^2 = p(h_k = 1) - [p(h_k = 1)]^2, \quad (24)$$

where $\mathcal{N}(\mu, \sigma^2)$ denotes the normal distribution. Thus, by using $\overline{C'_k}$ and its standard deviation,

$$\overline{\sigma_{C'_k}} = \sqrt{\frac{\overline{\sigma_1^2} + \overline{\sigma_2^2}}{S}}, \quad (25)$$

where $\overline{\sigma_1^2}$ and $\overline{\sigma_2^2}$ are the unbiased variances of $\ln p(h_k | \mathbf{v})$ and h_k in Eq. (21), respectively, we change the removal criterion from $C_k \leq 0$ into $\overline{C'_k} + a \overline{\sigma_{C'_k}} \leq 0$, where a tunes confidential intervals of C'_k .

In summary, our node removal procedure is as follows (Alg. 1). First, we remove all of the hidden units which satisfy the modified removal condition. Then, at each parameter update step, we choose the smallest removal cost and decrease it by using Eq. (17) until some hidden unit can be removed.

Algorithm 1 Node removal procedure

```

1: for number of removing iterations do
2:   repeat
3:     obtain  $S$  realizations,  $(\mathbf{v}^1, \mathbf{h}^1), \dots, (\mathbf{v}^S, \mathbf{h}^S)$ 
   by  $n$ -step block Gibbs sampling (PCD- $n$ ).
4:     evaluate  $\overline{C'_j}$  for all remaining hidden units by
   using Eq. (21).
5:     determine a node to be removed,  $k = \arg \min_j \overline{C'_j}$ .
6:     evaluate  $\overline{\sigma_{C'_k}}$  by using Eq. (25).
7:     if  $\overline{C'_k} + a\overline{\sigma_{C'_k}} \leq 0$  then
8:       remove the target node
9:       obtain  $S$  realizations by Gibbs sampling
   (tempered transition, from  $\beta_0 = 1$  to  $\beta_1$  divided by  $l$ 
   intervals).
10:    end if
11:    until  $\overline{C'_j} + a\overline{\sigma_{C'_j}} > 0$  for any  $j$ .
12:    evaluate  $\overline{\partial_i D}, \overline{\partial_i C_k}, \overline{\sigma_{D,i}},$  and  $\overline{\sigma_{C,i}}$ .
13:    determine  $\overline{\Delta \xi}$  from Eq. (17).
14:     $\xi^{s+1} = \xi^s - \nu \overline{\Delta \xi}$ .
15: end for

```

IV. NUMERICAL SIMULATION

In this Section, we show that the proposed algorithm does not spoil the performance of RBMs by using two kinds of datasets. First, we used 3×3 Bars-and-Stripes dataset [38], which is small enough to allow us to calculate the exact KLD during the course of removal processes. Next, we employed MNIST dataset of handwritten images and verified that our algorithm also works in realistic size RBMs.

Since parameter update after sufficient learning slightly changes $p(\mathbf{v}, \mathbf{h})$, it can be considered that short Markov chains are enough for convergence to $p(\mathbf{v}, \mathbf{h})$ after parameter updates. Thus, we used PCD [23] with n -step block Gibbs sampling (PCD- n) in both learning and removal processes except for samplings immediately after a node removal. However, since change of $p(\mathbf{v}, \mathbf{h})$ caused by node removal is expected to be larger than that caused by parameter updates, PCD- n with small n may not converge to $p(\mathbf{v}, \mathbf{h})$ and may fail to sample from $p(\mathbf{v}, \mathbf{h})$ immediately after node removals. Thus, we carefully performed Gibbs sampling by using tempered transition [25, 39] at these times. In tempered transition, we linearly divided inverse temperature from $\beta_0 = 1$ to $\beta_1 = 0.9$ into $l = 100$ intervals.

A. Bars-and-Stripes

First, we trained the RBM with $M = 9$ visible units and $N = 30$ hidden units by using PCD-5 and PCD-1 with a batch size of 100 and a fixed learning rate $\lambda = 10^{-2}$. Then, we performed removal processes starting from the same trained RBM with a batch size of 1,000 and fixed parameter change rate, $\nu = 10^{-2}$. Our removal criterion was $\overline{C'_k} + 3\overline{\sigma_{C'_k}} \leq 0$.

The results are shown in Figs. 2, 3, and 4. We stopped the removal processes at 10,000,000th step in Fig. 2 and at 5,000,000th step in Figs. 3, and 4. The removal procedure employed PCD-5 slowly decrease N with small fluctuations of the KLD in all five trials (Fig. 2). In particular, the removal cost in Fig. 2 shows that if a hidden unit whose removal cost is the smallest is removed before decreasing it, the KLD increases by about seven times, which shows usefulness of the update rule, Eq. (17), to keep the performance during node removal processes. The removal procedure employed PCD-1 decrease N more rapidly while approximately preserving the KLD in six out of eight trials (Fig. 3), although some peaks appear in the change of the KLD after node removals. However, two out of eight trials employed PCD-1 fail to preserve the KLD (Fig. 4).

First, we discuss the peaks which arose in Fig. 3. These peaks are resulted from inaccurate estimates of C'_k or $\overline{\Delta \xi}$. In order to distinguish them, we enlarge peaks in the change of the KLD (Fig. 5) and find that these peaks were caused by the failure of Gibbs sampling in parameter updates immediately after node removals rather than node removals themselves. This behavior supports the intuition that the change of $p(\mathbf{v}, \mathbf{h})$ caused by node removal can be large and can result in failure of Gibbs sampling, although most of the parameter updates after node removal produced small peaks, due to the tempered transition.

Next, we discuss large fluctuations of the KLD in Fig. 4. Failure of Gibbs sampling through parameter updates is expected to occur more frequently as the removal process continues for the same reason in the learning process [27, 40]. In the learning process, absolute values of ξ_i 's are considered to become large, in order to adjust $p(\mathbf{v})$, which is an almost uniform distribution at the beginning of training, to $q(\mathbf{v})$. In the removal process, $|\xi_i|$'s of remaining nodes are also considered to increase by parameter update in order to compensate roles of hidden units to be removed. Since block Gibbs sampling behaves almost deterministically in large $|\xi_i|$'s, dependence on initial condition remains for a long time, or equivalently, it takes a long time for convergence to $p(\mathbf{v}, \mathbf{h})$ after one-step parameter update. Thus, the difference between

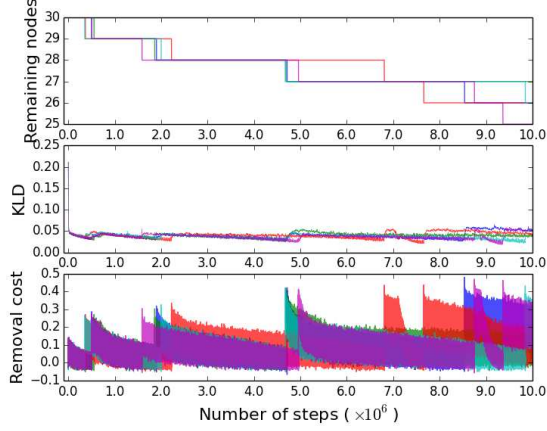


FIG. 2. The number of hidden units N (upper), the KLD (middle), and the smallest removal cost (lower) are shown as the functions of the number of removal steps. As a dataset, 3×3 Bars-and-Stripes was employed. We used PCD-5 for block Gibbs sampling. Each color in upper and lower figures corresponds to each trial.

$p(\mathbf{v}, \mathbf{h})$ after parameter update and the probability distribution after few block Gibbs sampling becomes large, and as a result, parameters are updated based on inaccurate Gibbs sampling estimates. If these deviations are corrected by subsequent parameter updates, D decreases again. However, if the failure of Gibbs sampling continues for a long time, the performance drastically fluctuates. From Fig. 4, it can be found that such a drastic decrease of the performance can emerge not only immediately after node removal (green line) but also sufficiently after removal (blue line). Therefore, in order to prevent the problem which stems from a long convergence time of Markov Chain Monte Carlo, the removal process should be stopped at some point in time as with the learning process.

B. MNIST

We first trained the RBM with $M = 784$ visible units and $N = 500$ hidden units by using PCD-1 with a batch size of 1,000 and a fixed learning rate $\lambda = 10^{-2}$. Then, we performed removal processes starting from the same trained RBM with a batch size of 1,000 and a fixed parameter change rate, $\nu = 10^{-2}$. Our removal criterion was $\overline{C'_k} + \overline{\sigma C'_k} \leq 0$.

As we have mentioned in Sec. 2, the KLD cannot be evaluated, owing to unknown probability $q(\mathbf{v})$ and large state space of the RBM. Thus, we employed two alternative evaluation criteria: One is the KLD

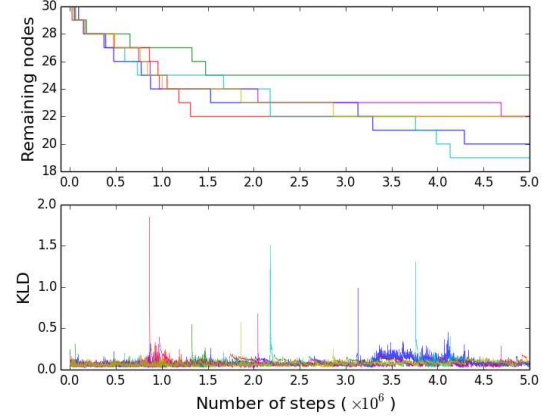


FIG. 3. The number of hidden units N (upper), and the KLD (lower) are shown as the functions of the number of removal steps. As a dataset, 3×3 Bars-and-Stripes was employed. We used PCD-1 for block Gibbs sampling. Each color in upper and lower figures corresponds to each trial.

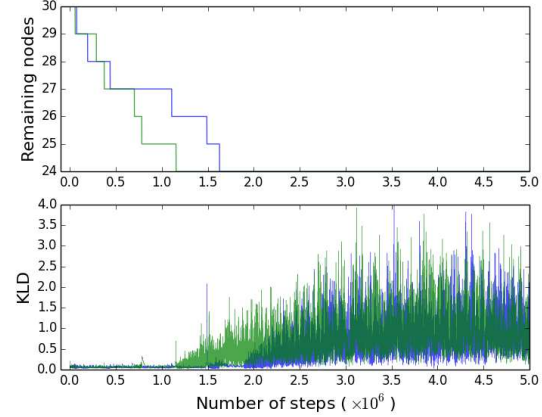


FIG. 4. Two trials failed to keep the KLD in case of PCD-1. Large fluctuation of the KLD emerged from immediately after node removal (green) and sufficiently after removal (blue).

of $p(\mathbf{v})$ from empirical distribution, $q_d(\mathbf{v})$,

$$\begin{aligned}
 \tilde{D} &\equiv D_{\text{KL}}(q_d || p) \\
 &= \sum_{\mathbf{v}} q_d(\mathbf{v}) \ln q_d(\mathbf{v}) + \ln Z \\
 &\quad + \sum_{\mathbf{v}} q_d(\mathbf{v}) \left[\sum_i b_i v_i \right. \\
 &\quad \left. + \sum_j \ln \left(1 + e^{c_j + \sum_i v_i w_{ij}} \right) \right], \quad (26)
 \end{aligned}$$

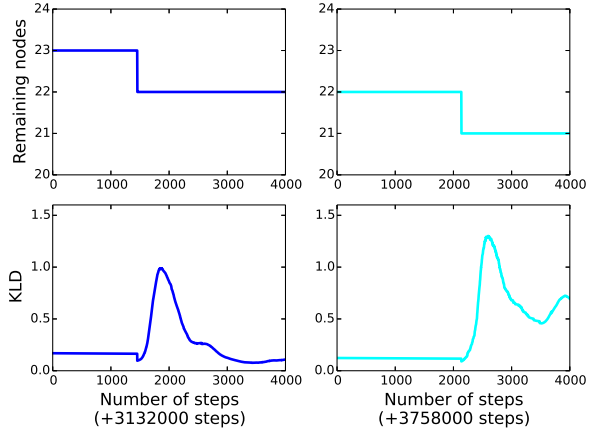


FIG. 5. The peaks after 3,000,000th (blue line) and before 4,000,000th steps (cyan line) in Fig. 3 are enlarged. These figures show that node removal slightly decreases the KLD, and parameter updates immediately after removal caused increases of the KLD.

where Z is the normalization constant of $p(\mathbf{v})$ and was evaluated by annealed importance sampling (AIS) [41]. The other is reconstruction error, R , which is widely used to roughly estimate performance of the RBM [28–30]:

$$R = -\frac{1}{S} \sum_{\alpha=1}^S \sum_{i=1}^M [v_i^\alpha \ln \tilde{v}_i^\alpha + (1 - v_i^\alpha) \ln(1 - \tilde{v}_i^\alpha)], \quad (27)$$

$$\tilde{v}_i^\alpha = \frac{e^{b_i + \sum_j w_{ij} \tilde{h}_j^\alpha}}{1 + e^{b_i + \sum_j w_{ij} \tilde{h}_j^\alpha}}, \quad (28)$$

$$\tilde{h}_j^\alpha = \frac{e^{c_j + \sum_i v_i^\alpha w_{ij}}}{1 + e^{c_j + \sum_i v_i^\alpha w_{ij}}}, \quad (29)$$

where α denotes index of a mini-batch, and \mathbf{v}^α is a sample from $q_{\text{data}}(\mathbf{v})$. On one hand, \tilde{D} evaluated by AIS is considered to reflect the performance of RBMs with high precisions and takes a long time for calculation. On the other hand, R is not considered to reflect the change of the KLD precisely and takes short time for calculation. Therefore, in order to monitor the change of the performance, we employed \tilde{D} at each 5,000 step and used R during removal processes for reference.

The results are shown in Figs. 6 and 7, and it can be found that our algorithm effectively works in a realistic size RBM. We stopped three removal processes at 1,500,000th step. Behaviors of N and \tilde{D} in Fig. 6 are qualitatively similar to those of N and the KLD in Figs. 2 and 3, and hence, interpretation of the results is the same as the numerical simulation in the previous subsection. As we explained in the pre-

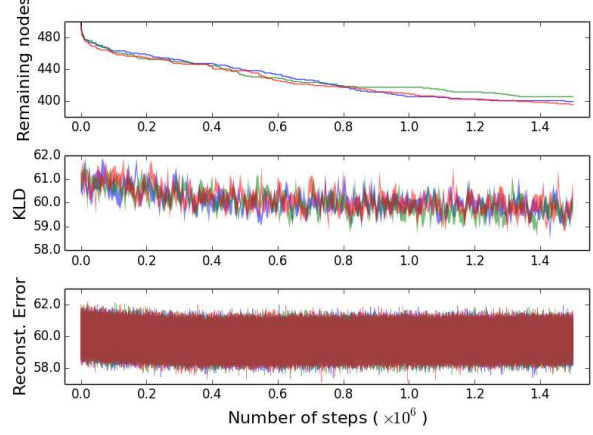


FIG. 6. The number of hidden units N (upper), the KLD of $p(\mathbf{v})$ from $q_{\text{data}}(\mathbf{v})$ (middle), and reconstruction error R (lower) are shown as the functions of the number of removal steps. MNIST handwritten images were employed as the dataset. Each color in upper, middle, and lower figures corresponds to each trial.



FIG. 7. MNIST images are shown at the start and the ends of the removal processes. The leftmost panel represents samples of visible configurations at 0th step of the removal processes, and the other three panels, from the left to the right, represent those at 1,500,000th step of the blue, green, and red lines in Fig. 6, respectively.

vious subsection, an extremely long removal process can increase $|\xi_i|$'s and may lead to failure of Gibbs sampling, which may successively increase the KLD. Thus, the removal process should be stopped before it spoils the performance. Since the KLD cannot be evaluated in large size RBMs, we recommend employing some evaluation criterion used in the learning process in Refs. [28–32] to monitor the change of the performance.

V. SUMMARY AND DISCUSSION

In this paper, we aim to decrease the number of hidden units of the RBM without spoiling its performance. For this purpose, we have introduced the removal cost of a hidden unit and have proposed a method to remove hidden units while avoiding drastic increase of the KLD. Then, we have applied the

proposed method to two kinds of datasets and have shown that the KLD were approximately kept during removal processes. The Increase of the KLD observed in the numerical simulations were caused by the failure of Gibbs sampling, which also becomes a problem in the learning process. The RBM has been confronting difficulties that how to accurately obtain expectation values which are computationally expensive. Researchers proposed many kinds of Gibbs sampling methods [22–27], which provide precise estimates and increase the performance of the RBM, although more accurate Gibbs sampling methods require a longer time for evaluations in general. If expectation values can be precisely evaluated, our algorithm is expected to work more effectively. We expect that physical implementation of the RBM [42] becomes an accurate and fast method for evaluation of the expectation values with respect to the probability distribution of an RBM.

Finally, since our algorithm can determine the target node to be removed by decreasing its contribution to the performance, repeating addition and removal of hidden units can replace whole hidden units of a system. Such procedure may be useful for reforming physically implemented systems which are hardly copied and must not be halted.

VI. ACKNOWLEDGMENT

This research is supported by JSPS KAKENHI Grant Number 15H00800.

$e^{-E(\mathbf{v}, \mathbf{h})}|_{h_k=0}$. Then, we can obtain C_k as follows:

$$\begin{aligned}
C_k &= D_{\text{KL}}(q||p_{\setminus k}) - D_{\text{KL}}(q||p) \\
&= \sum_{\mathbf{v}} q(\mathbf{v}) \ln \frac{q(\mathbf{v})}{\sum_{\mathbf{h}_{\setminus k}} p_{\setminus k}(\mathbf{v}, \mathbf{h}_{\setminus k})} \\
&\quad - \sum_{\mathbf{v}} q(\mathbf{v}) \ln \frac{q(\mathbf{v})}{\sum_{\mathbf{h}} p(\mathbf{v}, \mathbf{h})} \\
&= - \sum_{\mathbf{v}} q(\mathbf{v}) \ln \sum_{\mathbf{h}_{\setminus k}} p_{\setminus k}(\mathbf{v}, \mathbf{h}_{\setminus k}) \\
&\quad + \sum_{\mathbf{v}} q(\mathbf{v}) \ln \sum_{\mathbf{h}} p(\mathbf{v}, \mathbf{h}) \\
&= - \sum_{\mathbf{v}} q(\mathbf{v}) \ln \frac{\sum_{\mathbf{h}_{\setminus k}} p_{\setminus k}^*(\mathbf{v}, \mathbf{h}_{\setminus k})}{\sum_{\mathbf{v}', \mathbf{h}'_{\setminus k}} p_{\setminus k}^*(\mathbf{v}', \mathbf{h}'_{\setminus k})} \\
&\quad + \sum_{\mathbf{v}} q(\mathbf{v}) \ln \frac{\sum_{\mathbf{h}} p^*(\mathbf{v}, \mathbf{h})}{\sum_{\mathbf{v}', \mathbf{h}'} p^*(\mathbf{v}', \mathbf{h}')} \\
&= - \sum_{\mathbf{v}} q(\mathbf{v}) \ln \frac{\sum_{\mathbf{h}_{\setminus k}} p^*(\mathbf{v}, \mathbf{h})|_{h_k=0}}{\sum_{\mathbf{v}', \mathbf{h}'_{\setminus k}} p^*(\mathbf{v}', \mathbf{h}')|_{h_k=0}} \\
&\quad + \sum_{\mathbf{v}} q(\mathbf{v}) \ln \frac{\sum_{\mathbf{h}} p^*(\mathbf{v}, \mathbf{h})}{\sum_{\mathbf{v}', \mathbf{h}'} p^*(\mathbf{v}', \mathbf{h}')} \\
&= - \sum_{\mathbf{v}} q(\mathbf{v}) \ln \frac{\sum_{\mathbf{h}_{\setminus k}} p^*(\mathbf{v}, \mathbf{h})|_{h_k=0}}{\sum_{\mathbf{h}} p^*(\mathbf{v}, \mathbf{h})} \\
&\quad + \ln \frac{\sum_{\mathbf{v}', \mathbf{h}'_{\setminus k}} p^*(\mathbf{v}', \mathbf{h}')|_{h_k=0}}{\sum_{\mathbf{v}', \mathbf{h}'} p^*(\mathbf{v}', \mathbf{h}')} \\
&= - \sum_{\mathbf{v}} q(\mathbf{v}) \ln p(h_k = 0|\mathbf{v}) \\
&\quad + \ln p(h_k = 0). \tag{A1}
\end{aligned}$$

Next, consider simultaneous removal of several hidden units, $\mathbf{k}' = (k_1, \dots, k_r)$. Following similar calculation above, we can obtain removal cost:

$$\begin{aligned}
C_{\mathbf{k}'} &\equiv D_{\text{KL}}(q||p_{\setminus \mathbf{k}'}) - D_{\text{KL}}(q||p) \\
&= - \sum_{\mathbf{v}} q(\mathbf{v}) \ln p(h_{k_1} = \dots = h_{k_r} = 0|\mathbf{v}) \\
&\quad + \ln p(h_{k_1} = \dots = h_{k_r} = 0). \tag{A2}
\end{aligned}$$

In case of the RBM, the first term of Eq. (A2) can be simplified as

$$\begin{aligned}
C_{\mathbf{k}'} &= D_{\text{KL}}(q||p_{\setminus \mathbf{k}'}) - D_{\text{KL}}(q||p) \\
&= - \sum_{\mathbf{v}} q(\mathbf{v}) \sum_{\alpha=1}^r \ln p(h_{k_\alpha} = 0|\mathbf{v}) \\
&\quad + \ln p(h_{k_1} = \dots = h_{k_r} = 0). \tag{A3}
\end{aligned}$$

Appendix A: Derivation of Eq. (11)

For convenience, we introduce two unnormalized probabilities, $p^*(\mathbf{v}, \mathbf{h}) = e^{-E(\mathbf{v}, \mathbf{h})}$ and $p_{\setminus k}^*(\mathbf{v}, \mathbf{h}_{\setminus k}) =$

Appendix B: Change of D and C_k by naive update rule, Eq. (12)

In this Appendix, we show that the naive update rule, Eq. (12), decreases both D and C_k at $\mathcal{O}(\Delta\xi)$. The change of D and C_k by Eq. (12) at $\mathcal{O}(\Delta\xi)$ are given by

$$\frac{\partial D}{\partial \xi_i} \Delta \xi_i = -\nu \cdot \theta \left(\frac{\partial D}{\partial \xi_i} \frac{\partial C_k}{\partial \xi_i} \right) \times \left(\frac{\partial D}{\partial \xi_i} \right)^2, \quad (B1)$$

$$\frac{\partial C_k}{\partial \xi_i} \Delta \xi_i = -\nu \cdot \theta \left(\frac{\partial D}{\partial \xi_i} \frac{\partial C_k}{\partial \xi_i} \right) \times \frac{\partial D}{\partial \xi_i} \cdot \frac{\partial C_k}{\partial \xi_i}. \quad (B2)$$

In case of $\partial D / \partial \xi_i \cdot \partial C_k / \partial \xi_i \geq 0$, Eqs. (B1) and (B2) become

$$\frac{\partial D}{\partial \xi_i} \Delta \xi_i = -\nu \cdot \left(\frac{\partial D}{\partial \xi_i} \right)^2 \leq 0, \quad (B3)$$

$$\frac{\partial C_k}{\partial \xi_i} \Delta \xi_i = -\nu \cdot \frac{\partial D}{\partial \xi_i} \cdot \frac{\partial C_k}{\partial \xi_i} \leq 0, \quad (B4)$$

and in case of $\partial D / \partial \xi_i \cdot \partial C_k / \partial \xi_i < 0$, Eqs. (B1) and (B2) become

$$\frac{\partial D}{\partial \xi_i} \Delta \xi_i = 0, \quad (B5)$$

$$\frac{\partial C_k}{\partial \xi_i} \Delta \xi_i = 0. \quad (B6)$$

Thus, in both cases, Eqs. (B1) and (B2) take non-positive values, and this update rule decreases both D and C_k at $\mathcal{O}(\Delta\xi)$.

[1] Y. Bengio, A. Courville, and P. Vincent, IEEE transactions on pattern analysis and machine intelligence **35**, 1798 (2013).

[2] K. He, X. Zhang, S. Ren, and J. Sun, in *Proceedings of the IEEE conference on computer vision and pattern recognition* (2016) pp. 770–778.

[3] A. Vaswani, N. Shazeer, N. Parmar, J. Uszkoreit, L. Jones, A. N. Gomez, L. Kaiser, and I. Polosukhin, in *Advances in Neural Information Processing Systems* (2017) pp. 6000–6010.

[4] I. Goodfellow, J. Pouget-Abadie, M. Mirza, B. Xu, D. Warde-Farley, S. Ozair, A. Courville, and Y. Bengio, in *Advances in neural information processing systems* (2014) pp. 2672–2680.

[5] A. v. d. Oord, S. Dieleman, H. Zen, K. Simonyan, O. Vinyals, A. Graves, N. Kalchbrenner, A. Senior, and K. Kavukcuoglu, arXiv preprint arXiv:1609.03499 (2016).

[6] J. Hestness, S. Narang, N. Ardalani, G. Diamos, H. Jun, H. Kianinejad, M. Patwary, M. Ali, Y. Yang, and Y. Zhou, arXiv preprint arXiv:1712.00409 (2017).

[7] S. Han, J. Pool, J. Tran, and W. Dally, in *Advances in neural information processing systems* (2015) pp. 1135–1143.

[8] Y. Guo, A. Yao, and Y. Chen, in *Advances In Neural Information Processing Systems* (2016) pp. 1379–1387.

[9] Y. Cheng, D. Wang, P. Zhou, and T. Zhang, arXiv preprint arXiv:1710.09282 (2017).

[10] M. Berglund, T. Raiko, and K. Cho, *Neural Networks* **64**, 12 (2015).

[11] M. B. Christopher, *PATTERN RECOGNITION AND MACHINE LEARNING*. (Springer-Verlag New York, 2016).

[12] P. Smolensky, *Information processing in dynamical systems: Foundations of harmony theory*, Tech. Rep. (COLORADO UNIV AT BOULDER DEPT OF COMPUTER SCIENCE, 1986).

[13] A. Fischer and C. Igel, in *Iberoamerican Congress on Pattern Recognition* (Springer, 2012) pp. 14–36.

[14] H. Larochelle and Y. Bengio, in *Proceedings of the 25th international conference on Machine learning* (ACM, 2008) pp. 536–543.

[15] G. E. Hinton and R. R. Salakhutdinov, *science* **313**, 504 (2006).

[16] G. E. Hinton, S. Osindero, and Y.-W. Teh, *Neural computation* **18**, 1527 (2006).

[17] R. Salakhutdinov and H. Larochelle, in *Proceedings of the thirteenth international conference on artificial intelligence and statistics* (2010) pp. 693–700.

[18] G. Carleo and M. Troyer, *Science* **355**, 602 (2017).

[19] J. Tubiana and R. Monasson, *Physical review letters* **118**, 138301 (2017).

[20] N. Le Roux and Y. Bengio, *Neural computation* **20**, 1631 (2008).

[21] The RBM whose visible and hidden units take $\mathbf{v}' \in \{-1, 1\}^M$ and $\mathbf{h}' \in \{-1, 1\}^N$ can be related to the RBM that takes $\mathbf{v} \in \{0, 1\}^M$ and $\mathbf{h} \in \{0, 1\}^N$ by changing parameters, $W' = W/4$, $b'_i = b_i/2 + \sum_j w_{ij}/4$ and $c'_j = c_j/2 + \sum_i w_{ij}/4$, where \mathbf{b}' , \mathbf{c}' and W' are biases and weight matrix of the RBM whose nodes take $\{-1, 1\}$.

[22] G. E. Hinton, *Neural computation* **14**, 1771 (2002).

[23] T. Tieleman, in *Proceedings of the 25th international conference on Machine learning* (ACM, 2008) pp. 1064–1071.

[24] T. Tieleman and G. Hinton, in *Proceedings of the 26th Annual International Conference on Machine Learning* (ACM, 2009) pp. 1033–1040.

[25] R. R. Salakhutdinov, in *Advances in neural information processing systems* (2009) pp. 1598–1606.

[26] K. Cho, T. Raiko, and A. Ilin, in *Neural Networks (IJCNN), The 2010 International Joint Conference on* (IEEE, 2010) pp. 1–8.

[27] G. Desjardins, A. Courville, Y. Bengio, P. Vincent, and O. Delalleau, in *Proceedings of the thirteenth international conference on artificial intelligence and statistics* (2010) pp. 145–152.

[28] Y. Bengio, P. Lamblin, D. Popovici, and H. Larochelle, in *Advances in neural information processing systems* (2007) pp. 153–160.

[29] G. W. Taylor, G. E. Hinton, and S. T. Roweis, in *Advances in neural information processing systems* (2007) pp. 1345–1352.

[30] G. E. Hinton, in *Neural networks: Tricks of the trade* (Springer, 2012) pp. 599–619.

[31] G. Desjardins, Y. Bengio, and A. C. Courville, in *Advances in neural information processing systems* (2011) pp. 2501–2509.

[32] D. Buchaca, E. Romero, F. Mazzanti, and J. Delgado, arXiv preprint arXiv:1312.6062 (2013).

[33] Minimization of the size of the RBM, which we do not discuss in this paper, can be expressed as follows. Find a set of parameters ξ that maximize the number of hidden units whose removal costs are zero subject to $D = D_0$, where D_0 is the KLD to be preserved. Since this problem is apparently difficult to solve, we greedily remove a hidden unit one by one in this paper.

[34] In case of $\nabla_\xi D = \mathbf{0}$, which seldom occurs in numerical simulations, we employ higher derivatives of D , and seek a direction along which both C_k and D decrease. By restricting the number of parameters to be updated, one can alleviate computational cost caused by a large number of the elements of higher order derivatives.

[35] D. H. Ackley, G. E. Hinton, and T. J. Sejnowski, in *Readings in Computer Vision* (Elsevier, 1987) pp. 522–533.

[36] R. Salakhutdinov and G. E. Hinton, in *AISTATS*, Vol. 1 (2009) p. 3.

[37] When zero divided by zero appears owing to rounding error, we approved this update by setting $z_i = 1$ in numerical simulations in Sec. 4.

[38] D. J. MacKay and D. J. Mac Kay, *Information theory, inference and learning algorithms* (Cambridge university press, 2003).

[39] R. M. Neal, *Statistics and computing* **6**, 353 (1996).

[40] A. Fischer and C. Igel, in *International Conference on Artificial Neural Networks* (Springer, 2010) pp. 208–217.

[41] R. M. Neal, *Statistics and computing* **11**, 125 (2001).

[42] V. Dumoulin, I. J. Goodfellow, A. C. Courville, and Y. Bengio, in *AAAI*, Vol. 2014 (2014) pp. 1199–1205.